

# SHAPES OF HOT AND ROTATING NUCLEI STUDIED WITH THE HECTOR ARRAY\*

ADAM MAJ

H. Niewodniczański Institute of Nuclear Physics  
Radzikowskiego 152, 31-342 Kraków, Poland

(Received February 5, 2001)

Results from a number of GDR experiments aiming at the investigation of hot nuclear shapes in two very different mass regions and performed with the HECTOR array are presented. For  $A=46$  Jacobi shapes at high angular momenta were observed. For  $A=216$  indications of large deformations at angular momenta close to the fission limit were found.

PACS numbers: 21.10.Re, 24.30.Cz, 25.70.Gh

## 1. Introduction

The Giant Dipole Resonance (GDR), coherent small-amplitude oscillations of protons against neutrons, was found to be a very good probe of nuclear shapes. This is because the shape of the GDR strength function reflects the average nuclear quadrupole deformation: in spherical nuclei the strength function can be described by a single Lorentzian function, whereas in deformed nuclei the strength function splits into 2 or 3 components, reflecting the oscillations along the major axes of the nucleus (see *e.g.* [1]). The size of this energy splitting is proportional to the deformation parameter  $\beta$ . In addition, the  $\gamma$ -decay of the GDR from highly excited states is very fast, so it can compete with other modes of nuclear decay, and therefore can provide the information on the initial stages of excited nuclei. During the last 10 years the study of highly excited and rotating nuclei through the investigation of the  $\gamma$ -decay of the GDR has been developed considerably, both experimentally as well as theoretically (see *e.g.* [2–7] and references therein).

---

\* Presented at the XXXV Zakopane School of Physics “Trends in Nuclear Physics”, Zakopane, Poland, September 5–13, 2000.

A sizable contribution to this progress was provided by the Copenhagen-Milan-Cracow collaboration, based on exclusive experiments performed with the HECTOR array (see Sec. 2). The carried investigations were concentrated mainly on the following aspects: the shape and thermal shape fluctuations, the origin of the GDR width, the properties of some “exotic” nuclei (super-deformation, heavy and super-heavy nuclei, Jacobi shapes) and on “entrance channel” effect in compound nucleus formation. The main achievements are summarized below.

The hot nuclei do not have a well defined shape, as it is the case for the cold nuclei, but they do fluctuate. These fluctuation can affect the measured quantities, as the GDR strength function and angular distribution. The extend of this fluctuations, their dependence on temperature and angular momentum, and their influence on the measured quantities were investigated in many nuclei [8–12].

The observed energy width of the GDR was found to arise from the interplay of two effects: the thermal shape fluctuations, which are controlled by the nuclear temperature, and the deformation effects, controlled by the angular momentum. In addition it was found, that the “collisional damping” effects, giving rise to the intrinsic GDR width, does not depend on temperature [13–15].

The GDR  $\gamma$ -decay from hot super-heavy nucleus  $^{272}\text{Hs}$  was possible to be observed for the first time [16, 17]. The studies have shown, that the fission process is slow enough, so there is time for collective modes to build-up. It was possible to extract the information on the lifetime of such hot super-heavy system, and on its effective shape.

It was possible, for the first time, to observe the low energy component of the GDR built on the superdeformed discrete band in  $^{143}\text{Eu}$  [18, 19]. From the intensity of this component it was concluded, that the superdeformation is the property of rather cold nuclei.

The influence of the entrance channel effect of the compound nucleus formation was investigated [20, 21]. The experimental results suggest a possibility of the pre-equilibrium emission of  $\alpha$ -particles at high angular momenta in the case of symmetric reaction. Such an emission populates the compound nucleus at different excitation energy and angular momentum, as compared to the case of asymmetric reaction.

This paper concentrates on results concerning the “exotic” shapes at high angular momenta of nuclei from two very different mass regions. In Sec. 3 are shown the results of the search for Jacobi shapes in  $^{46}\text{Ti}$  nuclei. Sec. 4 contains the preliminary results of the experiment concerning the shapes of  $^{216}\text{Rn}$  nuclei.

## 2. The HECTOR array

The HECTOR (High-Energy  $\gamma$ -ray deteCTOR) array was built in 1989 as a Danish–Italian collaboration. The essential part of the array consists of 8 large volume scintillators of  $\text{BaF}_2$  for the detection of high-energy photons and 38 smaller hexagonal  $\text{BaF}_2$  crystals that serve as multiplicity filter (called HELENA) for the low-energy  $\gamma$ -transitions. The details can be found in [8]. HECTOR was originally located at the Tandem Accelerator Laboratory of the NBI (Denmark). It has operated there until 1998, when it was moved to the LNL at Legnaro (Italy).

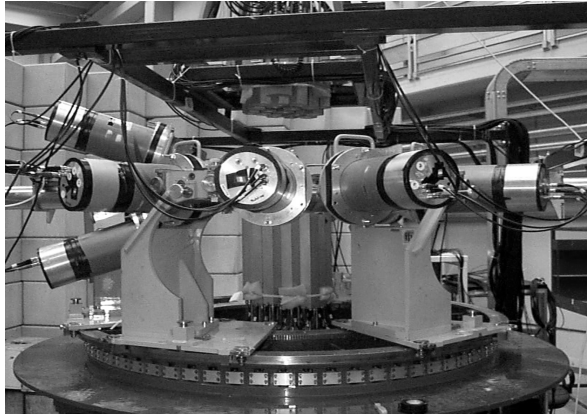


Fig. 1. The HECTOR set-up in LNL Legnaro (photo by F. Camera).

It was there upgraded by the Milano–Cracow–Copenhagen collaboration, and operates since then. Fig. 1 shows the photography of the present set-up. Four carriages, each of them carrying two  $\text{BaF}_2$  detectors, placed on the correlation table, can be precisely moved around the target and fixed at any angle. A pair of detectors in each carriage can be arranged either in horizontal plane ( $\phi = 0^\circ$ ) or out of horizontal plane ( $\phi = \pm 18^\circ$ ), depending on the experiment's needs. Such a construction gives the flexibility to set up different types of experiments.

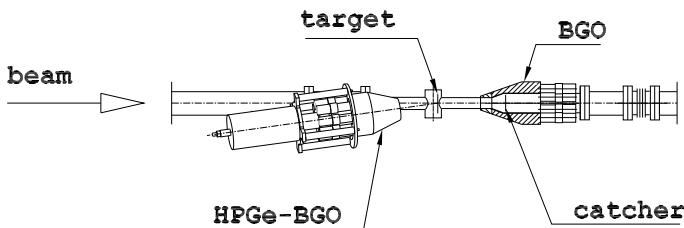


Fig. 2. The extension of the HECTOR set-up used for the recoil-catcher experiments.

It can also be easily extended by inserting additionally auxiliary detectors. Fig. 2 shows, for example, the catcher set-up added to the standard HECTOR configuration for the experiment discussed in Section 4. The HECTOR detectors were also used in conjunction with the large Ge-arrays (NORDBALL, PEX, EUROBALL) [18, 19].

### 3. Search for Jacobi shapes in light nuclei

In the search for exotic nuclear shapes, the light- and medium-mass nuclei are of special interest. This is because these nuclei are expected to undergo a Jacobi shape transition (from oblate via triaxial to very elongated prolate) at values of the angular momentum which are relatively low and below the fission limit. For example for nuclei with mass  $A \approx 45$  the critical angular momentum for the Jacobi transition is expected to be around  $29 \hbar$ .

The experimental signatures for Jacobi shapes for  $A \approx 45$  nuclei would be a pronounced high energy bump at  $E_\gamma \approx 25$  MeV in the strength function of the GDR together with a rather large anisotropy. In particular the anisotropy should be characterized by negative values of the  $A_2$  coefficient below  $E_\gamma \approx 18$ – $19$  MeV and by positive values at higher transition energies.

The first experimental evidence for the Jacobi shape transition was obtained by the Seattle group [23] for the  $^{45}\text{Sc}$  compound nuclei and it was based on inclusive spectra. In the photon absorption cross-section a shoulder at  $E_\gamma \approx 25$  MeV was found which becomes more and more visible with increasing bombarding energy. This has suggested large effective deformation of the compound system at high rotational frequencies. However, the corresponding  $A_2$  coefficient of the angular distributions did not show the expected behavior.

In order to search for the Jacobi transition effect, and to explain the unexpected behaviour of the measured angular anisotropy, we have studied the GDR decay from the hot and rotating  $^{46}\text{Ti}$  nucleus populated in the  $^{18}\text{O} + ^{28}\text{Si}$  reaction at 98 MeV, using the accelerator facility of the Niels Bohr Institute at Risø (Denmark). The compound nucleus  $^{46}\text{Ti}$  was produced with the excitation energy of 81 MeV, and with angular momentum distribution with  $l_{\text{max}} \approx 32 \hbar$ . The high-energy  $\gamma$ -rays were measured as a function of the multiplicity filter's fold at different angles [27].

Fig. 3 shows the experimental results for the 2 fold regions. The upper row displays the measured spectra in the logarithmic scale, together with the results of the statistical model fit. The calculations assumed that the GDR strength function is of double Lorentzian type. To examine the details of the GDR strength function, the experimental spectra were converted into our best estimate of the photon absorption cross-section and shown in a linear scale in the middle row of Fig. 3. This GDR cross-section is represented by

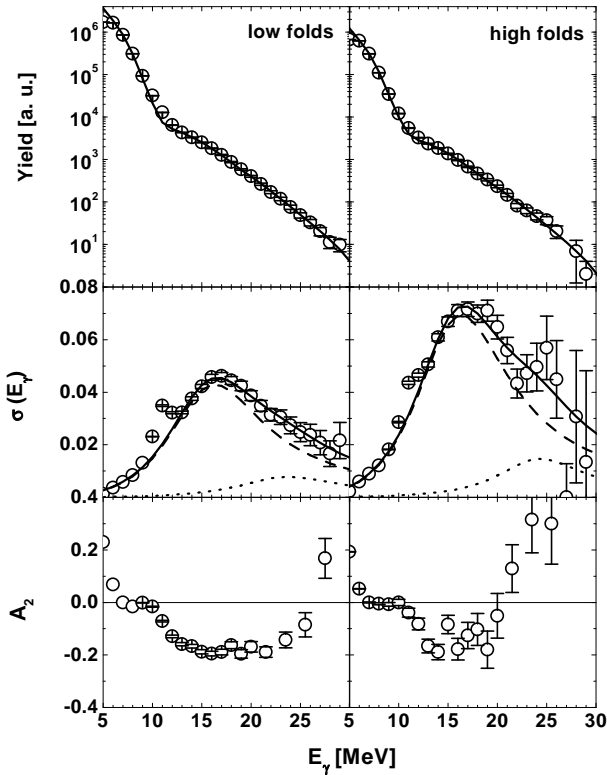


Fig. 3. Results from the measurement of the GDR  $\gamma$ -decay from  $^{46}\text{Ti}^*$ . Upper row: experimental spectra (in logarithmic scale) for low (5–6) and high (9–11) fold regions (points) and results of the CASCADE code fits (lines). Middle row: the photo-absorption cross-section determined from the fits (solid lines) together with the two Lorentzian components (dashed lines); and photo-absorption cross-section extracted from the measured spectra (points). Bottom row: experimental spectra of the  $A_2$  coefficient of the angular distributions.

the expression  $F_{2L} \times Y_{\text{exp}}/Y_{\text{fit}}$ . In this expression  $Y_{\text{exp}}$  is the experimental spectrum and  $Y_{\text{fit}}$  is the calculated spectrum assuming that the GDR decay can be represented by the double Lorentzian function  $F_{2L}$ , the latter being the best fit to the experimental spectrum. For the data gated by high folds one can note a shoulder at around  $E_\gamma \approx 24$  MeV, similar to that seen in the  $^{45}\text{Sc}$  nucleus [23]. The quadrupole deformation parameter deduced from the centroids of the 2 fitted Lorentzian components is  $\beta \approx 0.4$ . Such a splitting could be consisted with the Jacobi shapes. The spectra of the  $A_2$  coefficient from the angular distribution extracted from the data are displayed in the bottom row of Fig. 3. For the low folds data the data

are negative in both regions of the low and high energy GDR components, showing a similar behaviour found in  $^{45}\text{Sc}$ . In contrast, for the highest fold window, the behaviour of the  $A_2$  coefficient changes and follows the expectation namely of being negative for the low energy component and positive for the high one. A possible explanation for the peculiar behaviour of the  $A_2$  distributions for lower folds (and for the inclusive data of Seattle group) could be existence in the spectra of low multiplicity component, for example from incomplete fusion.

In order to understand why only for the highest folds the data are showing both the expected shoulder in the GDR strength function, and the correct angular distribution behaviour, one has to note that in light nuclei the preferred decay is via evaporation of charged particles. This can remove substantial amounts of angular momentum from the compound system.

This is illustrated in Fig. 4, where the calculated population distributions of the residual nuclei are shown. In the calculations it was assumed that the initial compound nucleus was populated at given angular momentum bin. For the heavier nucleus, as for example  $^{147}\text{Eu}$  (upper row), the different initial spins of compound nucleus are correlated with different angular momentum distributions of final nuclei (hence different measured folds). For

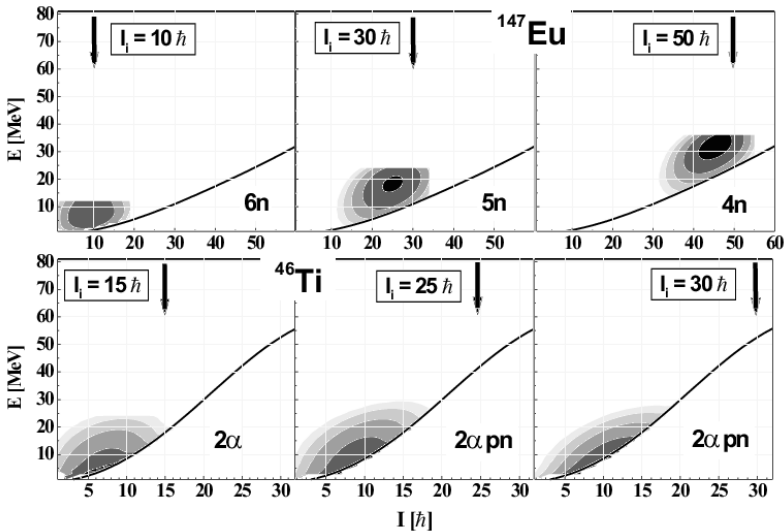


Fig. 4. Calculated population distributions of residual nuclei in the dominant evaporation channel on  $E^*$  vs  $I$  plane, as a function of the initial angular momentum  $I_i$  of the  $^{147}\text{Eu}$  (upper row) and  $^{46}\text{Ti}$  compound nuclei. One can see that in the  $^{46}\text{Ti}$  case the population distribution (which determines the measured fold distribution) is almost insensitive to  $I_i$ .

the light nucleus  $^{46}\text{Ti}$  (bottom row) however, the final distributions are almost the same. Therefore the measurement of high-energy  $\gamma$ -rays associated with low-fold and medium-fold coincidences of low-energy  $\gamma$ -rays is rather insensitive to the angular momentum of the decaying system, and contains contribution both from low and high angular momenta. Only when gating on very high-fold coincidences (corresponding to high  $\gamma$ -multiplicity) one is favouring the selection of the events originating mainly from the highest angular momenta of the compound nucleus. The high folds region corresponds to angular momentum of  $30 \pm 5 \hbar$ , indeed probing the region where Jacobi transition is expected to appear.

A simple estimate of the type of the effective shape probed by the giant dipole oscillation can be obtained by comparing the measured quantities (strength function and  $A_2$ ) with the calculations corresponding to the fixed deformation parameter  $\beta = 0.4$ , as obtained from the statistical model fit. These calculations, representing a first level analysis, are shown in Fig. 5 in comparison with the experimental quantities. Two of them correspond to axially symmetric shapes:  $\gamma = 0^\circ$  (collectively rotating prolate shape) and  $\gamma = -60^\circ$  (oblate, non-collective rotation). The third calculation is for the 3-axial shape with  $\gamma = -30^\circ$ . In the case of the GDR strength function one

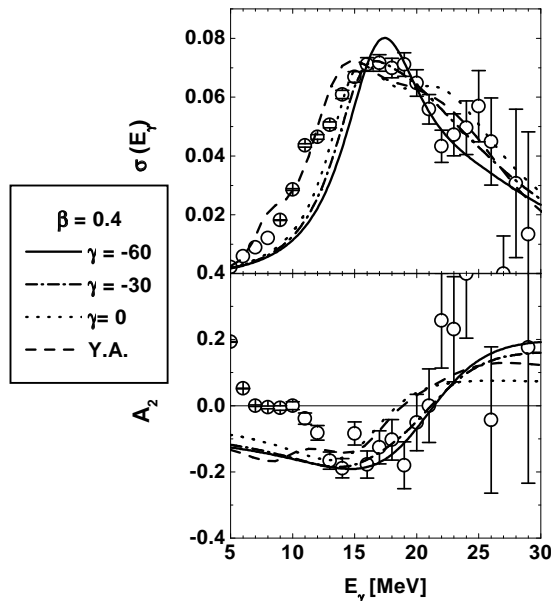


Fig. 5. Experimental cross-section and  $A_2$  spectra for the highest fold window together with simple calculations assuming 3 different nuclear shapes, with the same deformation parameter  $\beta$ , but different non-axiality parameters. Also the results from the thermal shape fluctuation model of Y. Alhassid are shown.

can rule out the oblate shape (upper part of Fig. 5) while in the case of the  $A_2$  coefficient (bottom part of Fig. 5) one sees that the prolate shape is the one that gives the worst fit to the data. Consequently, altogether these very simple estimates suggest that these  $^{46}\text{Ti}$  nuclei have an effective deformation with  $\beta \approx 0.4$  and of triaxial type with  $\gamma \approx -30^\circ$ , corresponding to the ratio of major axes 1.6 : 1.25 : 1. These shapes are those expected for nuclei undergoing the Jacobi shape transition. Additionally, the prediction based on the model including thermal shape fluctuations and in which the Jacobi instability is visible [24], are shown in the Fig. 5 as long dashed line. They also can reproduce the experimental findings, supporting the indication of Jacobi shapes present at high angular momenta.

#### 4. Shapes of hot Radon nuclei close to the fission limit — isomer tagged GDR spectra

Nuclei possessing large angular momenta, in the vicinity of the fission barrier, are expected to have large deformations. So far, the problem of shapes in fissioning nuclei has been studied with measurements in which GDR  $\gamma$ -decay was detected in coincidence with the fission fragments (post-fission) and from the fissioning nuclei (pre-fission) [16, 17, 25]. The analysis and the interpretation of such experiments is however difficult, since the measured spectra contain contribution both from the GDR decay in the fissioning nucleus and in the fission fragments.

It is therefore clear that measurements associated with nuclei close to the fission barrier but surviving the fission competition are extremely interesting since they allow to study the nuclear shapes in a new regime and in spectra free from fission fragments contribution. In addition, measurements of this type are important to test the model of thermal shape fluctuations in this extreme regime close to the fission, not yet explored.

In the experiment performed with the HECTOR array in LNL-Legnaro we made use of long-lived high-spin isomeric states in  $^{212}\text{Rn}$  ( $I^\pi = 30^+$ ,  $T_{1/2} = 154\text{ ns}$ ) and  $^{211}\text{Rn}$  ( $I^\pi = 63/2^-$ ,  $T_{1/2} = 201\text{ ns}$ ) to tag the GDR decay from the angular momentum region close to the fission limit [27]. The basic idea of the experiment was to use the recoil-catcher geometry technique, similar to that previously employed in discrete  $\gamma$ -spectroscopy of the Polonium isotopes [28] or in the GDR studies of Dysprosium isotopes [29].

The compound nucleus  $^{216}\text{Rn}$  was formed in the 96 MeV  $^{18}\text{O}$  on  $^{198}\text{Pt}$  reaction with the angular momentum distribution with  $I_{\text{max}} \approx 40\hbar$ . The value of the maximum angular momentum imparted by the reaction exceeds slightly the fission limit expected to be around  $35\hbar$ . Therefore one can expect that the decay path of the compound nucleus in competition with fission feeds strongly those isomeric states. Consequently, the detection

of high-energy  $\gamma$ -rays in coincidence with the delayed radiation from the isomers allows to select Rn nuclei at the angular momenta close to the fission limit, but still surviving the fission competition.

Fig. 2 illustrates the catcher set-up added to the standard HECTOR configuration. A self-supported target  $^{198}\text{Pt}$  ( $1\ \mu\text{g}/\text{cm}^2$  thick), where compound nucleus was formed and the prompt  $\gamma$ -radiation took place, was surrounded by the HECTOR array (8 large volume  $\text{BaF}_2$  detectors and a multiplicity filter). The residual nuclei, ejected from the target, were stopped in a thin ( $\approx 6\ \mu\text{m}$ ) Mylar catcher, having central 6 mm hole for the beam. The catcher was positioned in the forward direction at a distance of 40 cm from the target, reached by the recoiling nuclei in about 150 ns. The delayed radiation emitted by the stopped residues was detected in a BGO detector — a conventional BGO anti-Compton shield inserted on the beam tube, so that it was surrounding the catcher in order to maximize the detection efficiency. A germanium detector in a BGO shield, installed at  $146^\circ$ , measured the discrete  $\gamma$ -radiation. The prompt high-energy  $\gamma$ -rays from the target were recorded on tape only when followed by the delayed radiation detected in the catcher set-up. In order to measure the coincidences between the prompt and delayed radiation we used a pulsed  $^{18}\text{O}$  beam, with a repetition period of 400 ns and a pulse width of 10 ns. Additionally, we measured the time between the reaction and the isomeric decay, and the sum energy of the delayed  $\gamma$  transitions. Fig. 6 shows the time spectrum of the radiation from the catcher relative to the prompt radiation from the target, so it corresponds to the recoils time of flight convoluted with the isomeric decay curve. In order to select the high-energy  $\gamma$ -rays feeding the longest isomeric

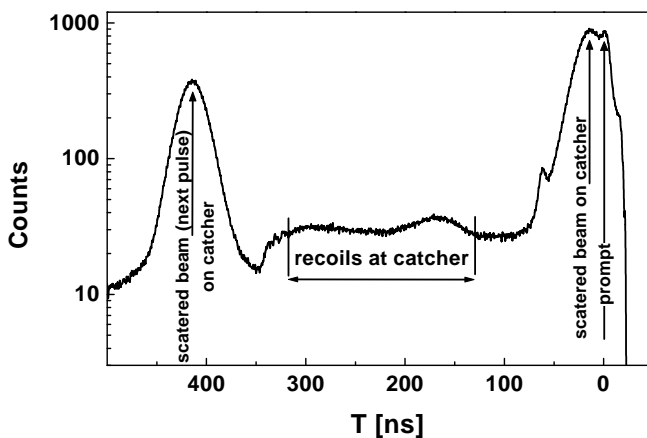


Fig. 6. Time spectrum of the  $\gamma$ -radiation measured in the BGO detector surrounding the catcher, relative to the prompt radiation. The gate used for Ge and  $\text{BaF}_2$  spectra is indicated as horizontal arrow.

states, a gate on the TOF spectrum was set, as shown in Fig. 6. To check, whether such a gate causes an enhancement of feeding to high-spin states, it was also used for gating Ge spectra.

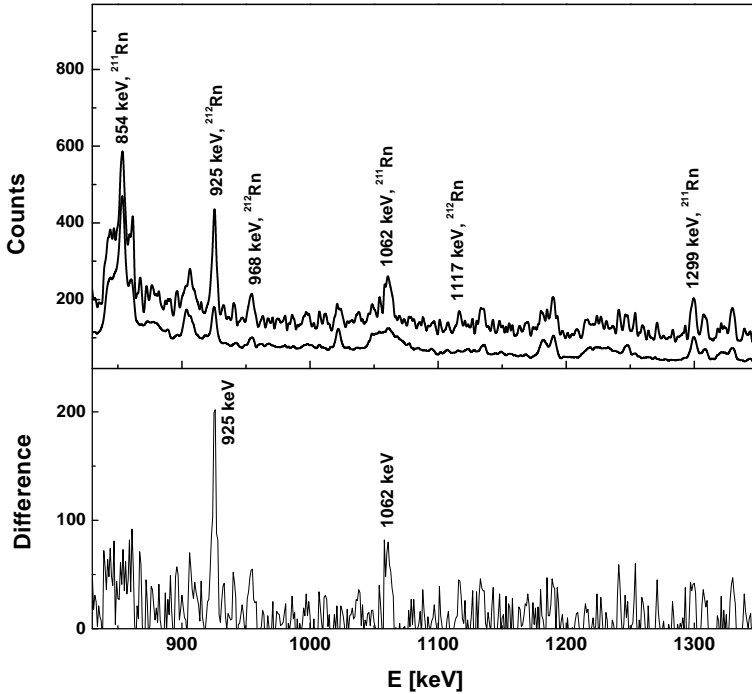


Fig. 7. Ge spectra: gated by the delayed  $\gamma$ -radiation (upper spectrum in the top panel), total (lower spectrum in the top panel) and their difference (bottom panel).

Fig. 7 shows Ge spectra: the total and the TOF-gated (normalized to 854 keV line) and their difference. In the latter spectrum the expected enhancement of the high-spin states feeding is clearly seen. Indeed, the 1062 keV line which feeds the  $63/2^-$  isomer in  $^{211}\text{Rn}$  and 924 keV which feeds the  $30^+$  isomer in  $^{212}\text{Rn}$  [26], are clearly enhanced.

Fig. 8 shows the total, ungated high-energy  $\gamma$ -spectrum (circles). In addition, the result from the statistical model fit to the total spectrum, assuming a single Lorentzian, is shown with the solid line. The calculation resulted in the GDR width of 10 MeV (see the inset in the Fig. 8), which is much larger than the ground state value ( $\approx 4$  MeV). This indicates, that even in the total spectrum larger deformations and thermal fluctuation effects are seen.

In the same figure the preliminary spectrum of high-energy  $\gamma$ -rays gated (as indicated in Fig. 6) by the isomeric decay is shown (squares). In addition,

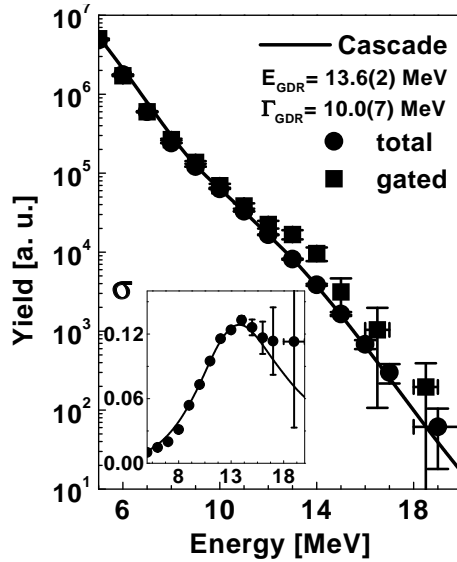


Fig. 8. High energy  $\gamma$ -spectra from the decay of  $^{216}\text{Rn}^*$ : circles — ungated spectrum; squares — spectrum gated by the delayed radiation; line statistical model fit to the ungated spectrum. In the inset: GDR photo-absorption cross-section as obtained from the statistical model fit to the ungated spectrum.

to obtain this spectrum it was required that the sum energy measured in the BGO detector was high enough to discriminate the low spin isomers and the background from the radioactivity. Both, gated and total spectra were normalized at 6 MeV. One notices, in spite of low statistics that the gated spectrum has relatively higher yield in the region  $E\gamma = 12\text{--}16$  MeV. This might indicate a larger contribution of prolate deformed shapes, as one would expect for nuclei on their way to fission.

However, a confirmation of that interpretation needs an analysis based on a Monte Carlo version of the statistical model code CASCADE. Such analysis is in progress and is expected to provide more quantitative information on the shapes of decaying  $^{216}\text{Rn}$  nuclei at very high spins.

## 5. Summary

The search of exotic shapes of nuclei induced by very fast rotation has been one of the very interesting subject both at  $T=0$  and at finite temperature.

The data here presented, obtained using the HECTOR array and concerning the  $^{46}\text{Ti}$  and  $^{212}\text{Rn}$  nuclei, have both shown the presence of large deformation. In particular, indication for the Jacobi transition is found in

the  $^{46}\text{Ti}$  case at high angular momenta. The high-energy spectra from the  $\gamma$ -decay of the GDR in hot Rn nuclei, gated by the isomers to enhance the feeding from the angular momentum region close to the fission barrier, also exhibit large effective deformations.

The more complete analysis of the present results together with the comparison with model predictions are expected to give a deeper insight to the interesting problem of nuclear shapes at finite temperature and very high spins.

This work is based on many experiments performed together with my colleagues from the HECTOR collaboration: A. Bracco, F. Camera, M. Mattiuzzi, B. Million and S. Leoni from Milano University; B. Herskind and J.J. Gaardhøje from the Niels Bohr Institute, Copenhagen; and M. Kmiecik from the Niewodniczański Institute of Nuclear Physics, Kraków. I would like to express my thanks to them. The fruitful discussions and the help in some of the experiments of W. Królas, W. Męczyński, J. Styczeń and M. Ziębliński from Kraków; and M. Kicińska-Habior, Z. Żelazny and J. Kownacki from Warsaw are acknowledged. This work was partly supported by the Polish State Committee for Scientific Research (KBN) Grant No. 2 P03B 001 16, the Danish Science Foundation and by the Italian Istituto Nazionale di Fisica Nucleare.

## REFERENCES

- [1] K.A. Snover, *Annu. Rev. Nucl. Part. Sci.* **36**, 545 (1986).
- [2] J.J. Gaardhøje, *Annu. Rev. Nucl. Part. Sci.* **42**, 483 (1992).
- [3] P.F. Bortignon, A. Bracco, R.A. Broglia, *Giant Resonances: Nuclear Structure at Finite Temperature*, Harwood Academic Publishers, 1998.
- [4] M. Kicińska-Habior, A. Maj, Z. Sujkowski, *Acta. Phys. Pol.* **B27**, 285 (1996).
- [5] P. Paul, M. Thoennessen, *Annu. Rev. Nucl. Part. Sci.* **44**, 65 (1994).
- [6] Y. Alhassid *et al.*, *Phys. Rev. Lett.* **65**, 2527 (1990).
- [7] W.E. Ormand *et al.*, *Nucl. Phys.* **A614**, 217 (1997).
- [8] A. Maj *et al.*, *Nucl. Phys.* **A571**, 185 (1994).
- [9] F. Camera *et al.*, *Nucl. Phys.* **A572**, 401 (1994).
- [10] W.E. Ormand *et al.*, *Phys. Rev. Lett.* **69**, 2905 (1992).
- [11] J.J. Gaardhøje *et al.*, *Acta Phys. Pol.* **B24**, 139 (1993).
- [12] M. Mattiuzzi *et al.*, *Phys. Lett.* **B364**, 13 (1995).
- [13] A. Bracco *et al.*, *Phys. Rev. Lett.* **74**, 3748 (1995).
- [14] M. Mattiuzzi *et al.*, *Nucl. Phys.* **A612**, 262 (1997).

- [15] M. Kmiecik *et al.*, *Nucl. Phys.* **A674**, 29 (2000).
- [16] A. Maj *et al.*, *Acta Phys. Pol.* **B26**, 417 (1995).
- [17] T.S. Tveter *et al.*, *Phys. Rev. Lett.* **76**, 1035 (1996).
- [18] F. Camera *et al.*, *Eur. Phys. J.* **A2**, 1 (1998).
- [19] F. Camera *et al.*, *Acta Phys. Pol.* **B32**, 807 (2001).
- [20] M. Kmiecik *et al.*, *Eur. Phys. J.* **A1**, 11 (1998).
- [21] A. Maj *et al.*, *Nucl. Phys.* **A649**, 137 (1999).
- [22] S. Cohen, F. Plasil, W.J. Świątecki, *Ann. Phys. (N.Y.)* **82**, 557 (1974).
- [23] M. Kicińska-Habior *et al.*, *Phys. Lett.* **B308**, 225 (1993).
- [24] Y. Alhassid, *Nucl. Phys.* **A569**, 37 (1994).
- [25] R. Butsch *et al.*, *Phys. Rev. Lett.* **41**, 1530 (1990).
- [26] G.D. Dracoulis *et al.*, *Phys. Lett.* **B246**, 31 (1990).
- [27] A. Maj *et al.*, *Nucl. Phys.* **A687**, 192 (2001).
- [28] A. Maj *et al.*, *Nucl. Phys.* **A509**, 413 (1990).
- [29] J.P.S. van Schagen *et al.*, *Nucl. Phys.* **A581**, 145 (1995).